RADIATION DAMAGE IN SILICON NIP SOLAR CELLS

I. Weinberg, C. Goradia*, C. K. Swartz,
and A. M. Hermann**
NASA Lewis Research Center
Cleveland, Ohio

INTRODUCTION

Solar cells with high base resisitivities have the potential, if properly designed, of providing high radiation tolerance. In the past however, radiation damage studies have been largely limited to cells with base resisitivities of 20 ohm-centimeters or less. Hence, because of the potential for increased radiation resistance, we have determined the performance parameters after 1-MeV electron irradiation of n^+ p p^+ silicon solar cells of varying thicknesses with boron-doped p-base resisitivities of 1250 and 84 ohm-centimeters. Although more appropriately described as n^+ p p^+, the higher resistivity cells approach the NIP condition. Because of the low majority carrier concentration in the base, a significant portion of the cell is in high injection under air mass zero (AMO) illumination. Thus high injection theory was used in analyzing the experimental data.

EXPERIMENTAL

The pre-irradiation cell characteristics are shown in table I. The cells were fabricated by Comsat under a program aimed, among other things, at demonstrating that high-quality, thin-high-resisitivity cells could be made using processing compatible with conventional practice (ref. 1). The cells were irradiated, at room temperature, by 1-MeV electrons to a maximum fluence of 10^{15} per square centimeter. Normalized short-circuit currents as a function of fluence are shown in figures 1 and 2, while normalized open circuit voltages are shown in figures 3 and 4.

ANALYSIS AND DISCUSSION

From figures 1 and 2, it is seen that the degradation in short-circuit current is small for the thinner cells in both resistivities. On the other hand, the highest degradation in I_{SC} occurs for the thickest 1250 ohm-centimeter cell. This phenomenon is associated with bulk resistivity and the absence of conductivity modulation occurring in high-injection (ref. 2). We are presently formulating a comprehensive theory of NIP solar cells which will be used in analyzing the complete cell characteristics. In

*NASA-ASEE Faculty Fellow. Permanent Address: Electrical Engineering Department, Cleveland State University, Cleveland, Ohio 44115.
**Temporary Employee. Present Address: Solar Energy Research Institute, Golden, Colorado 80401.

the absence of such a complete closed-form theory, we have limited ourselves, for the present to consideration of the open-circuit voltage. Our analysis is based on a theory which is valid for both low and high injection (ref. 3). A schematic diagram of the cell structure is shown in figure 2 where V_J and V_{JB} are the voltage developed across the front and back junctions, respectively, and V_B is the voltage drop across the cell base. For illumination from the n^+ side (ref. 3)

$$V_{oc} = V_J + V_{JB} - V_B \tag{1}$$

$$V_J = \frac{kT}{q} \ln \frac{I_{sc}}{I_o} \tag{2}$$

$$V_{JB} = \frac{kT}{q} \ln \left(1 + \frac{n_p(w)}{N_{ap}}\right) \tag{3}$$

$$V_B = \frac{kT}{q}\left(\frac{b-1}{b+1}\right) \ln \left(\frac{n_p(o) + \frac{bN_{ap}}{b+1}}{n_p(w) + \frac{bN_{ap}}{b+1}}\right) \tag{4}$$

In equation (4) $b = \mu_n/\mu_p$ where μ_n and μ_p are the mobilities of electrons and holes, respectively, in the base region, $n_p(o)$ and $n_p(w)$ are the base minority carrier concentrations at the front and back junctions, respectively, and N_{Ap} is the acceptor concentration in the base.

Typical results for the voltage components are shown in figures 6 and 7. Considering the components of V_{OC}, we note that V_J, the front junction potential for the 84 ohm-centimeter cell, is significantly greater than that for the 1250 ohm-centimeter cell. Analysis based on equation (2) indicates that this differential is due predominantly to a lower value of I_O the device saturation current, for the 84 ohm-centimeter cell. Considering V_{JB}, it is noted that the rear junction potential is several times greater for the 1250 ohm-centimeter cell than for the lower resistivity cell. Analysis based on equation (3) shows that this is due primarily to the decreased acceptor concentration in the 1250 ohm-centimeter cell. With respect to V_B, it is noted from the figures that this component increases with fluence, contrary to what is observed for the other components. Computation of the base minority carrier concentrations at the junctions show that these concentrations change with fluence. Hence, from equation (4), a change in the minority carrier distribution with fluence is responsible for the observed rise in V_B.

In computing the preceding voltage components, the base minority carrier diffusion length was treated as an adjustable parameter, thus yielding computed values of diffusion length. The resultant pre-irradiation values are shown in table II where the high-injection values correspond to the present AMO data, while the low-injection values were obtained using a low level X-ray excitation technique (ref. 4). Also shown in the table are

diffusion length damage coefficients K_L obtained for both the high and low injection conditions. A thickness-dependent diffusion length is noted in high injection, while the diffusion lengths for low injection are significantly smaller than those obtained under high injection. In addition, the damage coefficients for high injection are lower than those for low injection. We are at present unable to give a consistent explanation for the thickness dependence of the diffusion length. On the other hand the relative diffusion length values are consistent with a saturation of recombination centers under high injection conditions.

CONCLUSION

The present results, obtained from an analysis of open-circuit voltages, show a much greater contribution to V_{OC} from the back junction than is the case for the lower resisitivity ($\rho \leq 20$ ohm-centimeters) in common use. The base minority carrier distribution is seen to be significant in determining the contribution of V_B, the base contribution to V_{OC}. Although V_B is small, its value increases with increasing radiation fluence. In this connection, it is noted that, with illumination from the p^+ side, the sign of V_B becomes positive, and V_B itself becomes an additive term to V_{OC}.

Diffusion lengths determined under high injection conditions are significantly greater than those obtained under low injection, while damage coefficients under low injection are higher than these obtained under high injection conditions. Although additional analysis is required, this result appears to be consistent with a saturation of recombination centers under high injection.

REFERENCES

1. Allison, J. F.; Arndt, R. A.; and Muelenberg, A., Jr.: Thin n-i-p Radiation Resistant Solar Cell Feasability Study. NASA CR-159871, 1980.
2. Schwartz, R. J.; and Lundstrom, M. S.: Degradation of BSF Solar Cell Performance at High Intensity Due to a Loss of Base Conductivity Modulation. The Conference Record of the Fourteenth IEEE Photovoltaic Specialists Conference - 1980. IEEE, 1980, pp. 1392-1393.
3. Wu, C.-Y.; and Shen, W-Z: The Open Circuit Voltage of Back-Surface-Field (BSF) p-n Junction Solar Cells in Concentrated Sunlight. Solid State Electron., vol. 23, no. 3, Mar. 1980, pp. 209-216.
4. Rosenzweig, W.: Diffusion Length Measurements by Means of Ionizing Radiation," Bell Syst. Tech. J., vol. 41, no. 5, Sept. 1962, pp. 1573-1588.

TABLE I. - PRE-IRRADIATION CELL CHARACTERISTICS
[AR Coating; Ta_2O_5.]

Resistivity, ρ, ohm-cm	Thickness, t, μm	Open-circuit voltage, V_{oc}, mV	Short-circuit current, I_{sc}, mA	Fill factor, percent	Efficiency, percent	Number of cells
1250	61	577	128.9	74.8	10.3	2
1250	101	579	141.9	72.2	10.8	↓
1250	250	580	146.8	69.9	10.9	↓
85	56	589	130.5	75.4	10.6	↓
85	250	572	152.5	70.2	11.2	3

TABLE II. - DIFFUSION LENGTHS AND DAMAGE COEFFICIENTS

Resistivity, ρ ohm-cm	Thickness, t, μm	Diffusion length, L, μm		Damage coefficient, K_1	
		High injection[a]	Low injection[b]	High injection[a]	Low injection[b]
1250	61	859	224	4×10^{-12}	--------
1250	101	1075	220	5.2×10^{-12}	9×10^{-12}
1250	250	1667	219	5.7×10^{-12}	20×10^{-12}
84	56	610	130	8.4×10^{-12}	18×10^{-12}
84	250	914	155	12×10^{-12}	40×10^{-12}

[a]From AMO data.
[b]From X-ray data.

NORMALIZED SHORT-CIRCUIT CURRENT VS 1 MeV
ELECTRON FLUENCE FOR 84 OHM-CM N^+PP^+ CELLS

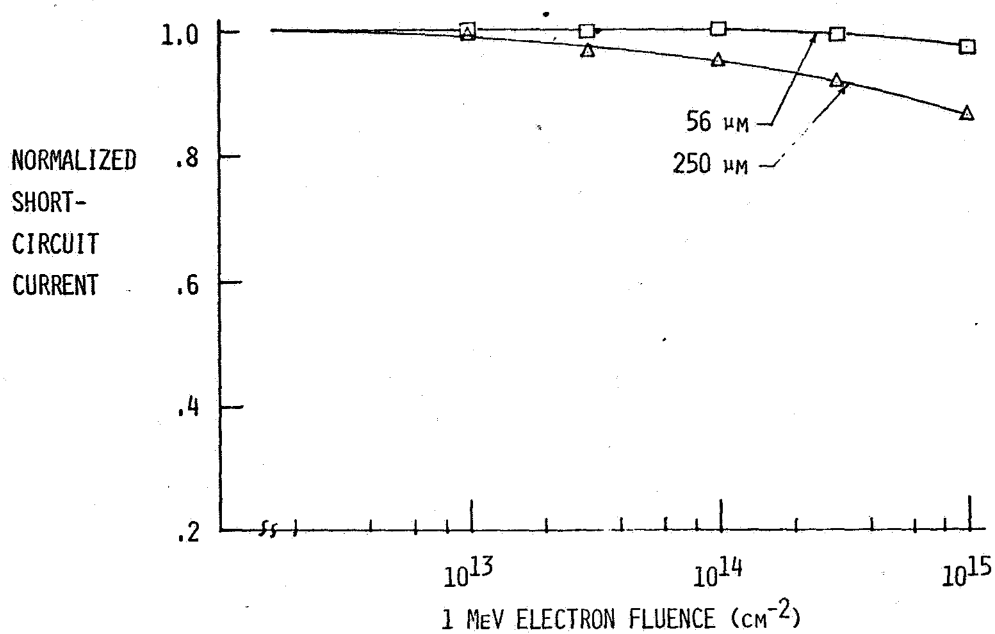

FIGURE 1

NORMALIZED SHORT-CIRCUIT CURRENT VS 1 MeV
ELECTRON FLUENCE FOR 1250 OHM-CM N^+PP^+ CELLS

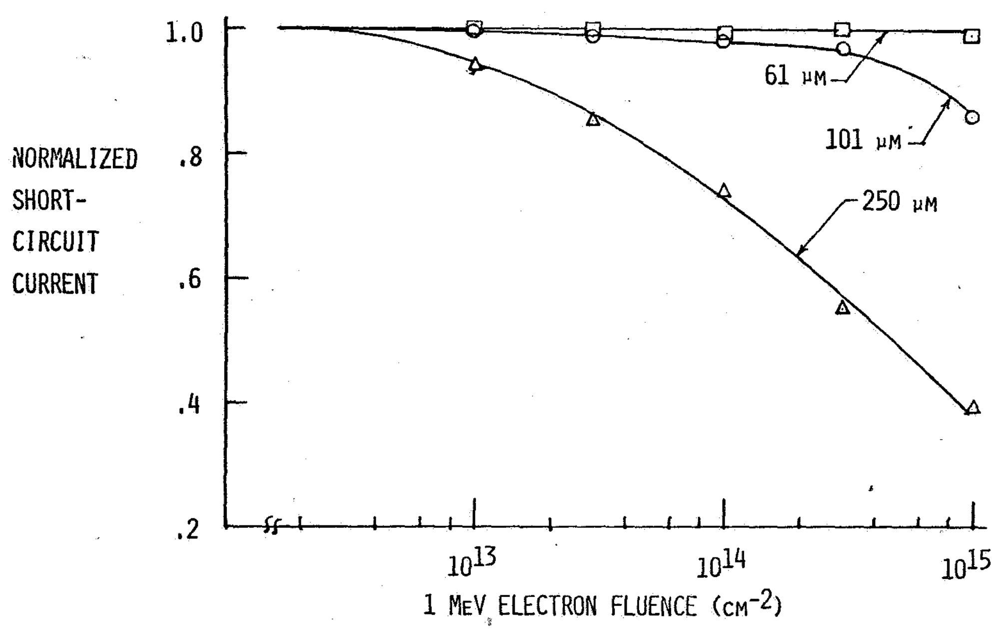

FIGURE 2

NORMALIZED OPEN-CIRCUIT VOLTAGE VS 1 MeV ELECTRON FLUENCE
FOR 84 OHM-CM N^+PP^+ CELLS

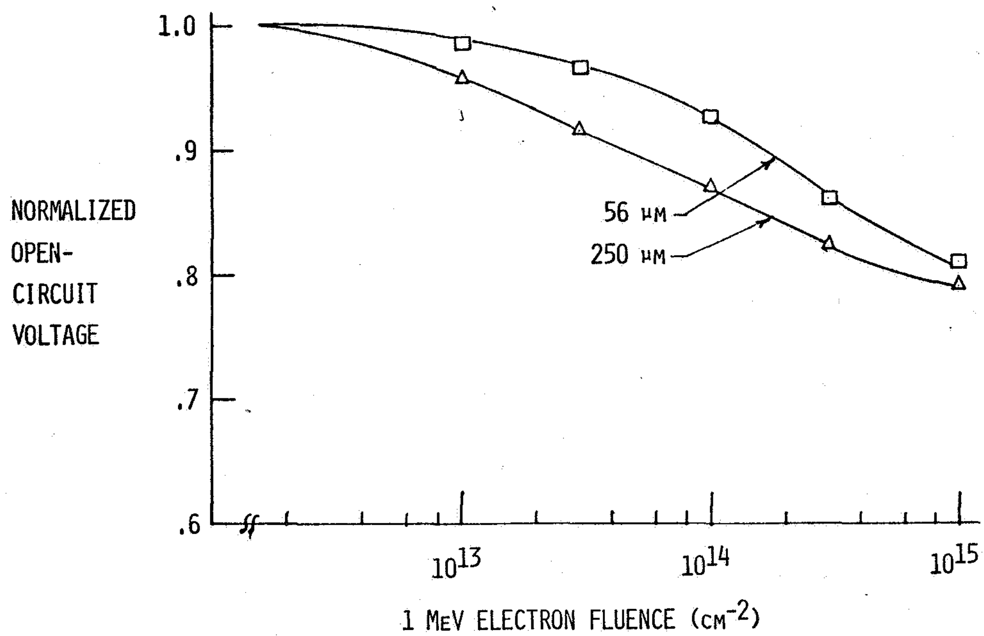

FIGURE 3

NORMALIZED OPEN-CIRCUIT VOLTAGE VS 1 MeV ELECTRON FLUENCE
FOR 1250 OHM-CM N^+PP^+ CELLS

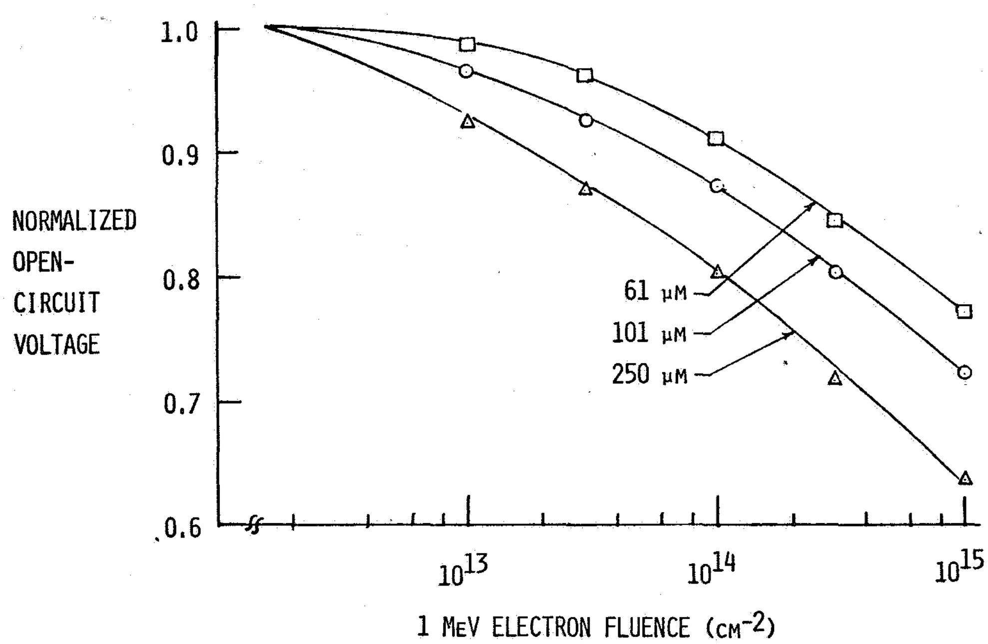

FIGURE 4

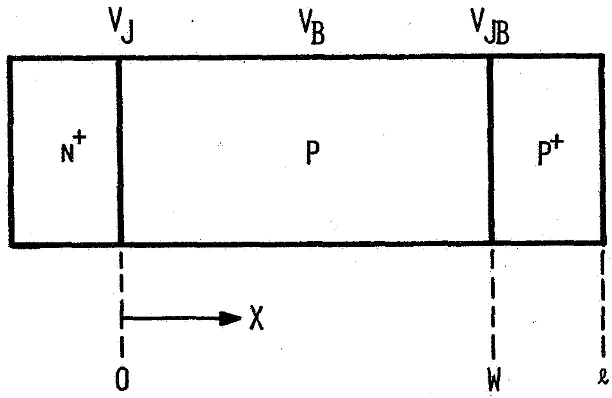

FIGURE 5

COMPONENTS OF OPEN-CIRCUIT VOLTAGE

FOR N^+PP^+ CELLS 1250 Ω-CM, 250 μM THICK

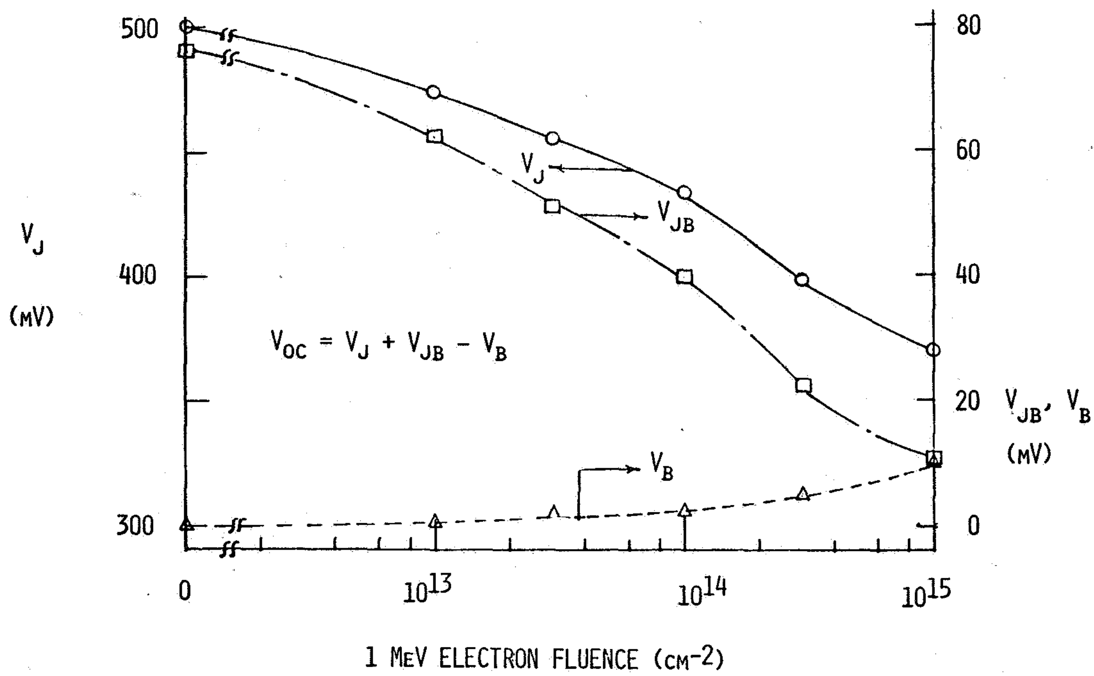

FIGURE 6

COMPONENTS OF OPEN-CIRCUIT VOLTAGE

FOR N^+PP^+ CELLS 84 Ω-CM, 250 μM THICK

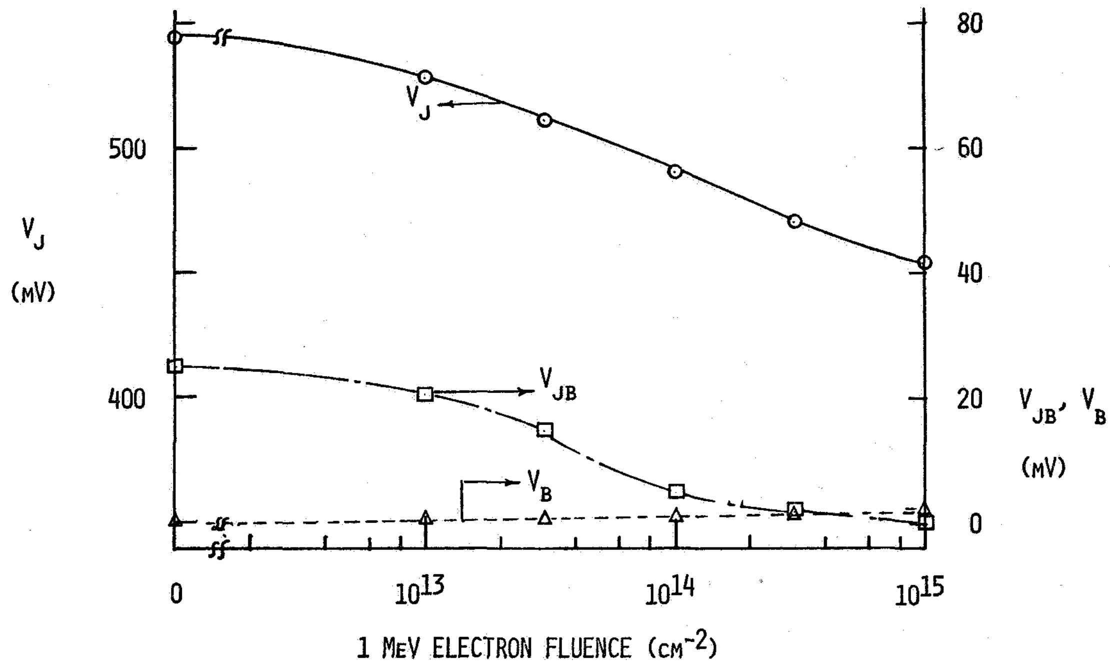

FIGURE 7